JOURNAL OF AGRICULTURAL AND FOOD CHEMISTRY

Immobilization of Fe Chelators on Sepharose Gel and Its Effect on Their Chemical Properties

ZEHAVA YEHUDA,† YITZHAK HADAR,‡ AND YONA CHEN*,†

Department of Soil and Water Sciences and Department of Plant Pathology and Microbiology, Faculty of Agricultural Food and Environmental Quality Sciences, The Hebrew University of Jerusalem, P.O. Box 12, Rehovot 76100, Israel

Iron chelates are usually costly and easily leached beyond the root zone. This creates a need to frequently replenish the rhizosphere with chelated Fe and might contaminate groundwater with organic compounds and metals. The development of a slow-release Fe fertilizer that will efficiently supply Fe to plants while exhibiting high resistance toward leaching and/or degradation in the rhizosphere has been the focus of this study. Desferrioxamine B (DFOB) and ethylenediaminebis(*o*-hydroxyphenylacetic acid) (EDDHA) were immobilized on Sepharose. ^{13}C NMR and FTIR measurements confirmed that coupling of DFOB to the gel did not appear to influence its ability to chelate Fe^{3+} or its binding nature. Isotherms for the immobilized ligands were determined in the presence of 1 mM HEDTA, at 25 °C and at an ionic strength of 0.1 M. The isotherms showed a high affinity of Fe^{3+} to the ligands and binding up to saturation level throughout the pH range examined (4.0−9.0). The K_{app} values for the immobilized Fe chelates were determined using a modified Scatchard model and found to be lower than the soluble ones. This decrease in K_{app} might facilitate Fe uptake from these chelates by plants.

KEYWORDS: Fe chelators; immobilization; stability constants; DFOB; EDDHA; Sepharose gel; Scatchard Plot; Fe binding isotherms

INTRODUCTION

The development of selective chelating resins has received much attention over the last few decades. The growing interest in chelating ion exchangers originates from their potential applications in analytical chemistry, metal processing, and wastewater treatment (*1*−*3*).

A suitable resin enriched with a metal-chelating agent for chemical and biological applications should possess a high capacity for, and a favorable selectivity toward, the metal, combined with high stability and a rapid exchange kinetics that will allow metal release and a recharge process. Most of the commercial resins exhibit a high capacity for, but poor selectivity toward, the metal ion (*4*). In some cases, the kinetics of complexation is slow, due to the hydrophobic characteristics of the polystyrene backbone. Quantifying functional groups of solid supported ligands is of high relevance to final product quality, selection of the appropriate solid support, and optimization of the coupling conditions of ligands via a selected protocol (*5*).

Iron chelators such as ethylenediaminebis(*o*-hydroxyphenylacetic acid) (EDDHA), diethylenetriaminepentaacetic acid (DTPA), and ethylenediaminetetraacetic acid (EDTA) are the most effective Fe fertilizers known to date. They are, however, easily leached beyond the depth of the root zone due to their negative charge (*6*, *7*). Besides the ecological aspect of contamination of groundwater with organic compounds and metals, leaching often creates the need to frequently replenish the rhizosphere with chelated Fe. Binding of the synthetic chelates or microbial siderophores to a solid phase is therefore an attractive alternative.

Aiming to overcome leaching, we studied sorption of various chelates on activated Sepharose gels. Although DFOB is positively charged at pH levels prevailing in calcareous soils, we selected it for this study as a model for microbial siderophores due to the large number of publications on this compound, its importance in the medical field, and its availability. In this study, DFOB and EDDHA will be immobilized on Sepharose. The influence of the coupling reaction on the Fe binding properties will be investigated to evaluate their function as an Fe source to plants.

THEORY: DETERMINATION AND CALCULATION OF STABILITY CONSTANTS

An important characteristic of a metal complex is its stability constant, the value of which provides an index of the affinity of the metal for the ligand. Stability constants are important factors required to predict the behavior of trace elements in the rhizosphere and their availability to plants. Chelates having high stability constants with Fe^{3+} may exhibit an improved potential to alleviate Fe deficiency in plants, although kinetics and the

* To whom correspondence should be addressed. Tel: 00972-8-9489234. Fax: 00972-8-9468565. E-mail: yonachen@agri.huji.ac.il.
† Department of Soil and Water Sciences.
‡ Department of Plant Pathology and Microbiology.

10.1021/jf034159h CCC: $25.00
Published on Web 08/28/2003

Fe^{3+} reducing potential are highly important factors (*7*−*9*). Below we will describe the theory and different approaches applied in this research for the determination of the stability constants for Fe^{3+} with DFOB and EDDHA sorbed on Sepharose gels.

Stability constants are classified according to the type of reaction they characterize. The overall reaction of a ligand L with a metal M is

$$nM + mL \rightleftharpoons M_nL_m \quad (1)$$

where *n* and *m* are the moles of metal ions and ligand molecules in the complex, respectively. The overall stability (equilibrium) constant (β_{ML}) is given by

$$\beta_{ML} = \frac{[M_nL_m]}{[M]^n[L]^m}$$

where brackets represent the concentration at a given ionic strength. The ligand and its metal complex may form various protonated species, based on protonation degree, possible M:L ratios, concentrations of the solution components, and, especially, pH. Each of these species has its own overall stability constant (*10*, *11*).

To simplify the comparison among chelators for their ability to compete for a specific metal in solution, across a wide concentration range, one should prefer the use of the term "apparent stability constant". The apparent stability constant (K_{app}) for a ligand L and a metal M is defined by

$$M^{n+} + L_t \rightleftharpoons ML_t \quad (2)$$

$$K_{app} = \frac{[ML_t]}{[M^{n+}][L_t]}$$

where L_t and ML_t represent the sums of all protonated and hydroxylated species of the ligand and its metal complex, respectively. K_{app} can be calculated for any given pH from all stepwise formation constants or from the overall stoichiometric stability constants (β) of all possible species, as described in the following equation for a 1:1 metal−ligand complex (*11*, *12*):

$$K_{app} = \frac{\beta_{ML} + \beta_{MLH}[H] + \beta_{MLH_2}[H]^2 + ...}{1 + \beta_{LH}[H] + \beta_{LH_2}[H]^2 + ...}$$

where all β values are the product of their partial stepwise stability constants (*K*):

$$\beta_{ML} = K_{ML} = \frac{[ML]}{[M][L]}$$

$$\beta_{MLH} = K_{MLH}{}^{H}K_{ML} = \frac{[MLH]}{[M][L][H]}, \text{ etc.}$$

(all charges omitted).

Nutrient cultures and soil solution are much more complicated systems than presented here. They contain various metals that might compete with Fe on the ligand as well as other competitive natural ligands. The equilibrium situation will depend on the K_{app} values of all ligands present, their concentrations, and the metal concentration. K_{app} accurately describes the affinity between a ligand and a given metal only when no other metals are present in the solution (*11*). It is stressed here that our discussion is confined to a system containing one metal and two ligands.

Ligand−Ligand Competition. Winston and Kirschner (*13*) reported the stability constants for several Fe^{3+} poly(hydroxamic) acids complexes measured by competition experiments between Fe^{3+}, the polymer, and EDTA. The procedure is based on the distribution of the metal between a soluble chelator and an insoluble chelating resin. When equilibrium is established, a definitive relationship should exist between the stability constants of the soluble and insoluble complexes. In practice, a suitable soluble chelator must be chosen to obtain a measurable distribution of metal between the resin and the soluble chelator.

Soluble hexadentate ligands such as DFOB and EDDHA form a 1:1 metal−ligand complex with Fe^{3+} (*14*). Assuming a 1:1 M:L ratio for the immobilized chelators as well, competition with a known soluble 1:1 complex will give rise to two chelation reactions:

$$M + L \rightleftharpoons ML \quad (3)$$

$$K = \frac{[ML]}{[M][L]}$$

$$M + L' \rightleftharpoons ML' \quad (4)$$

$$K' = \frac{[ML']}{[M][L']}$$

where M is the metal, L and L′ are the soluble and immobilized ligands, respectively, and ML and ML′ are the soluble and immobilized metal complexes, respectively. Brackets represent the concentration at a given ionic strength, and *K* and *K*′ are the equilibrium constants of reactions 3 and 4, respectively.

Assuming that L and L′ represent the sum of all protonated species of the soluble and immobilized ligands, respectively, and ML and ML′ are the sum of all protonated species of the soluble and immobilized metal complexes, respectively, at a given pH, then *K* and *K*′ will represent the K_{app} values (*11*, *12*) of the soluble and immobilized complexes, respectively.

A system including a metal and both soluble and immobilized ligands can be described as a combination of reactions 3 and 4:

$$ML + L' \rightleftharpoons ML' + L \quad (5)$$

$$K'' = \frac{[ML'][L]}{[ML][L']} = \frac{[ML'][M][L]}{[M][L'][ML]} = \frac{K'}{K}$$

Since *K* is known and *K*″ can be determined experimentally, *K*′, the apparent stability constant of the immobilized chelate, can be calculated from their multiplication. In eq 5 the total concentration of M is known. Since L and L′ have high affinities for M, and if their total concentrations are kept higher than that of M, it is reasonable to assume that no metal precipitation occurs and that the metal distributes between L and L′.

The mass equation for M is therefore (*13*)

$$[M]_t = [ML] + [ML'] \quad (6)$$

The soluble complex concentration [ML] can be measured and the concentration of the immobilized complex [ML′] calculated from eq 6. The ligand concentrations [L] and [L′] can be calculated from eqs 7 and 8, respectively.

$$[L_t] = [ML] + [L] \quad (7)$$

$$[L'_t] = [ML'] + [L'] \quad (8)$$

$[L_t]$ and $[L'_t]$ are the results of the preparation procedure.

Scatchard Analysis. The Scatchard analysis (*10*, *15*) has been used to evaluate the affinity constant and number of binding sites in various biological processes such as Fe nutrition in infants (*16*), disease factors (*17*), and medical treatments (*18*). Nir et al. (*19*) applied this method to the prediction of uptake of particles by cells and Stevenson (*10*) for the determination of metal humate complex. On the basis of work by Stevenson (*10*) and Nir et al. (*19*) we slightly modified Scatchard plots to evaluate the immobilized-ligand density on the solid matrix, [L′], and to determine its K_{app} value with Fe^{3+}.

Rearrangement of eqs 6 and 8 gives

$$[L'] = [L'_t] - [ML'] = [L'_t] - ([M]_t - [ML]) \qquad (9)$$

Multiplication of eq 10 by K'' yields

$$K''[L'] = K''[L'_t] - ([M]_t - [ML])$$

From eq 5

$$K''[L'] = \frac{[ML'][L]}{[ML]}$$

Therefore

$$\frac{[ML'][L]}{[ML]} = K''[L'_t] - K''([M_t] - [ML]) \qquad (10)$$

$$[L'_t] = G_0N \qquad (11)$$

where G_0 is the weight of the solid matrix on which the ligand L′ is immobilized and N is the molar concentration of metal-binding sites per gram of solid phase (gel in our study).

After eq 10 is divided by the initial concentration of the immobilized ligand, $[L'_t]$, eqs 10 and 11 yield

$$\frac{[ML'][L]}{G_0N[ML]} = K'' - (K''([M_t] - [ML])/G_0N) \qquad (12)$$

Following the literature (*10*, *15*, *19*), we define the metal bound to the solid matrix, m, as

$$m = ([M_t] - [ML]/G_0) \qquad (13)$$

With the introduction of m into eq 12 and multiplication by N, a linear relationship is obtained:

$$\frac{m[L]}{[ML]} = K''N - K''m \qquad (14)$$

where the slope of the curve is K'' and N can be calculated from the intercept of the curve. K'' is unitless and at a given pH is actually the ratio between the apparent stability constants K_{app} of the soluble and immobilized ligands (*10*, *20*, *21*).

MATERIALS AND METHODS

Preparation of Immobilized Chelates. Desferrioxamine B (DFOB (**Figure 1**), Desferal; Ciba Geigy, Basel, Switzerland) or ethylendiaminebis(*o*-hydroxyphenylacetic acid) (EDDHA (**Figure 2**), Sigma, St. Louis, MO), were immobilized on CNBr-activated Sepharose 4B and epoxy-activated Sepharose 6B (Pharmacia, Uppsala, Sweden) according to the manufacturer's instructions. The following activated Sepharose samples (Sigma, St. Louis, MO) were prepared in our laboratory: cyano transfer activated Sepharose (*22*), (*p*-nitrophenyl)chloroformate (PNPCF) activated Sepharose (*23*), PNPCF activated Sepharose with ϵ-aminocaproic acid as spacer arms (*24*), *O*,*N*-succinimidyl-*N*,*N*,*N*′,*N*′-tertramethyluronium tetrafluoroborate (TSTU) and (dimethylamino)-pyridine (DMAP) activated Sepharose (*23*).

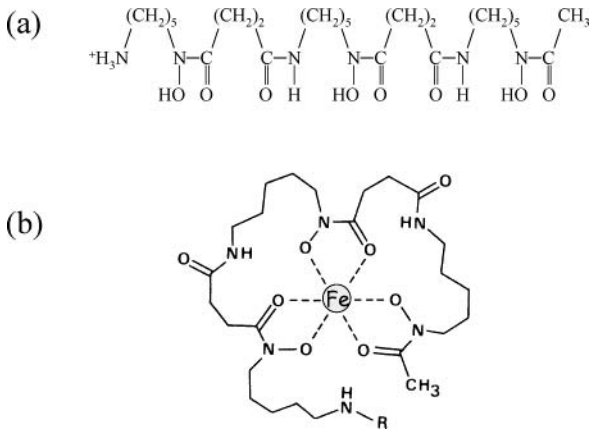

Figure 1. Chemical structures of (a) desferrioxamine B (DFOB) and (b) ferrioxamine B (FeDFOB).

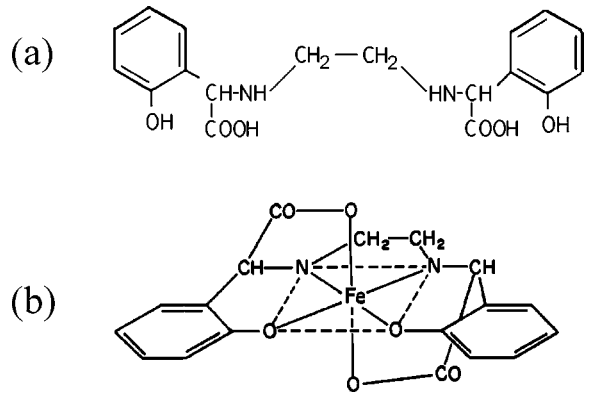

Figure 2. Chemical structures of (a) EDDHA (ethylenediaminebis(*o*-hydroxyphenylacetic acid)) and (b) FeEDDHA (S,S isomer).

Coupling the Ligand to the Activated Gel. DFOB and EDDHA were coupled to the activated gel in phosphate-buffered saline (PBS) or 50 mM HEPES (*N*-[2*H*]piperazine-*N*′-[2-ethanesulfonic acid], Sigma Chemical Co., St. Louis, MO) buffer at pH 7.4 at 4 °C with shaking. The ligand was added to the activated gel at a ratio of 3:1 v:w. After 2 days, $NaHCO_3$ was added to a final concentration of 0.1 M and shaken at 4 °C for another 2 days. The chelate−resin complex was washed with distilled water, 0.1 M NaOH, and 50 mM HEPES buffer at pH 7.4, freeze-dried under vacuum, and kept at −20 °C.

Fourier Transform Infrared (FTIR) Spectroscopy. The FTIR spectra of DFOB and EDDHA as free or immobilized ligand samples were obtained for a wavenumber range of 4000−400 cm^{-1} with a Nicolet 550 Magna-IR spectrometer (Nicolet Instruments Corp., Madison, WI). The samples were freeze-dried and finely ground prior to analysis. Samples for analysis were prepared by mixing and pounding 98−99 mg of KBr with 1−2 mg of the tested material and then compressing the mixture into pellets. To obtain FTIR spectra, 20 scans were collected. To compare one spectrum to another, a linear baseline correction was applied using 4000, 3700, 2600, 1800, and 800 cm^{-1} as zero-absorbance points. The major-peak data (intensity and wavenumber) were obtained by using OMNIC software (Nicolet Instruments Corp., Madison,WI).

Cross-Polarization and Magic Angle Spinning (CPMAS) Nuclear Magnetic Resonance (^{13}C NMR) Spectroscopy. Solid-state CPMAS ^{13}C NMR spectra were recorded using a Bruker DPX 300 MHz NMR spectrometer (Bruker Analytic GmbH). The spectrometer was operated at 100 and 25 MHz for ^{1}H and ^{13}C, respectively, with the following experimental parameters: contact time of 1 ms; recycle delay time of 0.8 s; sweep width of 28 kHz; line broadening of 0 Hz. Freeze-dried samples were placed into a 4 mm rotor and spun at a frequency of 3.5 kHz at the magic angle (54.7° to the magnetic field).

Table 1. Iron Chelating Capacity of the Immobilized Ligands Sorbed on Activated (Various Activation Procedures) Sepharose Gel

activation procedure	ligand	Fe chelating capacity (μM/g)
Commercial Activated Gels		
CNBr-activated Sepharose 4B	DFOB	38
	EDDHA	47
epoxy-activated Sepharose 6B	DFOB	59
	EDDHA	74
Sepharose CL 4B Activated in our Laboratory		
CNBr and triethylamine	DFOB	55
PNPCF[a] and DMAP[b]	DFOB	260
	EDDHA	285
PNPCF and DMAP with ϵ-aminocaproic acid as spacer arms	DFOB	51
TSTU[c] and DMAP with ϵ-aminocaproic acid as spacer arms	DFOB	46

[a] (*p*-Nitrophenyl)chloroformate. [b] (Dimethylamino)pyridine. [c] O,N-Succinimidyl-*N*,*N*,*N*′,*N*′-tertramethyluronium tetrafluoroborate.

Adsorption Isotherms. Increasing concentrations of Fe as $Fe(NO_3)_3$ were added to 10 mg of immobilized DFOB in the presence of 10^{-3} M citric acid or *N*-(2-hydroxyethyl)ethylenediaminetriacetic acid (HEDTA), for the comparison between the different activation procedures and the determination of K_{app}, respectively, to avoid precipitation of Fe as iron oxides. Solutions were adjusted to pH 4.0, 5.5 and 6.5, 7.3, and 9.0 using 50 mM glycine, MES, HEPES, and Tris buffers, respectively. An ionic strength of 0.1 M was maintained using KCl. The tubes were shaken for 24 h and 3 days for the comparison between the different activation procedures and the determination of K_{app}, respectively, at 25 °C. This is based on preliminary experiments, which showed that most of the Fe^{3+} was bound to the immobilized gel within 24 h and that no significant changes in Fe^{3+} concentration in the solution were detected between 3 day and 1 month equilibrium periods. The equilibrium concentrations of Fe in the solutions were determined by inductive coupled plasma (ICP) spectroscopy (Spectroflame modula E, Spectro, Kleve, Germany). The amount of Fe adsorbed to the immobilized ligand was calculated from the difference between total Fe concentration and that of the soluble Fe, assuming there was no Fe precipitation. The data were subjected to Scatchard analysis, and K' values were determined from the slope of the curve and from ligand-exchange competition according to eq 5.

RESULTS AND DISCUSSION

Activation Procedures. Several activation methods were tested on Sepharose followed by coupling of the ligand (DFOB or EDDHA) to the solid matrix. The activated Sepharose was compared to commercial activated gels. Capacities of the immobilized DFOB and EDDHA for Fe binding at pH 7.3 resulting from the various activation methods are summarized in **Table 1**. The highest ligand density after 24 h was achieved using PNPCF in the presence of DMAP as the activator. Although most widely used for the activation of hydroxyl group of a polymeric support, coupling of amines to CNBr-activated agarose forms unstable N-substituted iso-urea bonds (*25*). In addition, the iso-urea bonds are positively charged at physiological pH (pK = 9.4), thereby exhibiting ion-exchange behavior which could interfere with the biospecificity of the adsorbent (*26*). In contrast, activation with PNPCF forms reactive carbonates on the Sepharose, and reaction with amines results in stable and uncharged urethane derivatives (*23*).

Addition of ϵ-aminocaproic acid as a spacer arm reduced the Fe-binding capacity of the gel, probably as a result of the low mechanical stability of the attached ligand or due to steric hindrance. The differently activated Sepharose gels differed not only in their ligand density and capacity for Fe^{3+} but also in their affinity for Fe^{3+}, as indicated by the slopes of the binding isotherms (**Figure 3**). Thus we used PNPCF to activate Sepharose and coupled the ligand directly to the gel.

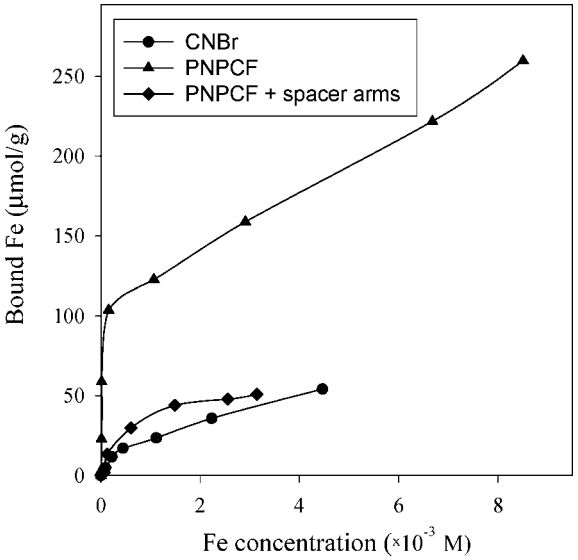

Figure 3. Binding isotherm of Fe^{3+} on immobilized DFOB (immobilization on activated Sepharose). Activation procedures: CNBr, cyanogen bromide activated Sepharose; PNPCF, (*p*-nitrophenyl)chloroformate activated Sepharose; PNPCF + spacer, PNPCF with ϵ-aminocaproic acid as spacer arms.

FTIR Analysis. The FTIR spectra of DFOB, immobilized DFOB, their complexes with Fe^{3+}, and Sepharose CL 4B are presented in **Figure 4**. The peaks at 3313 and 3102 cm^{-1}, which were assigned to N−H stretch bands overlapping with the strong O−H band of the hydroxamic groups, were clearly noticeable in the IR spectrum of DFOB. However, these peaks were completely shielded by the strong broad band around 3400 cm^{-1} of Sepharose hydrogen-bonded hydroxyl groups in the spectrum of immobilized DFOB. The C−H stretching of methylene groups appearing at 2931 and 2858 cm^{-1} and their bending vibrations in the range of 1400−1460 cm^{-1} could be distinguished in both spectra. Both DFOB and immobilized DFOB showed absorption at 1568 cm^{-1}. This absorption involves coupling of the N−H bending and C−N stretching vibrations of the secondary amide. The high-intensity signal of the DFOB hydroxamate C═O stretching at 1628 cm^{-1} and the peaks around 1656−1643 cm^{-1} resulting from C═O stretching of the agarose polymer in the spectrum of Sepharose were seen as one sharp peak at 1652 cm^{-1} in the immobilized DFOB spectrum. The DFOB sulfonamide peak appearing at 1196 cm^{-1} disappeared after coupling the ligand through its free amino group to the Sepharose. The peak at 1270 cm^{-1} and the C−N stretch bands at 1050−1170 cm^{-1} when DFOB was immobilized were hidden by the distinct broad peaks at 1159 and 1077 cm^{-1} assigned to C−O stretching of the Sepharose. These peaks, however, were shifted and split into four peaks at 1168, 1113, 1070, and 1045 cm^{-1} as a result of the new C−O bond formed upon activation of the Sepharose with PNPCF. The signals at frequencies of 1778, 1595, and 1520 cm^{-1} possibly resulted from the carbamate bond between the gel and the ligand.

Upon complexation of DFOB with Fe^{3+}, the most distinct changes were in the range of 3600−3100, 1650−1560 and 1078 cm^{-1}. The most pronounced peak was the one assigned to N−H of the secondary amide at 3440 cm^{-1}. The shift in this peak could be attributed to the dissociation of the hydroxamate

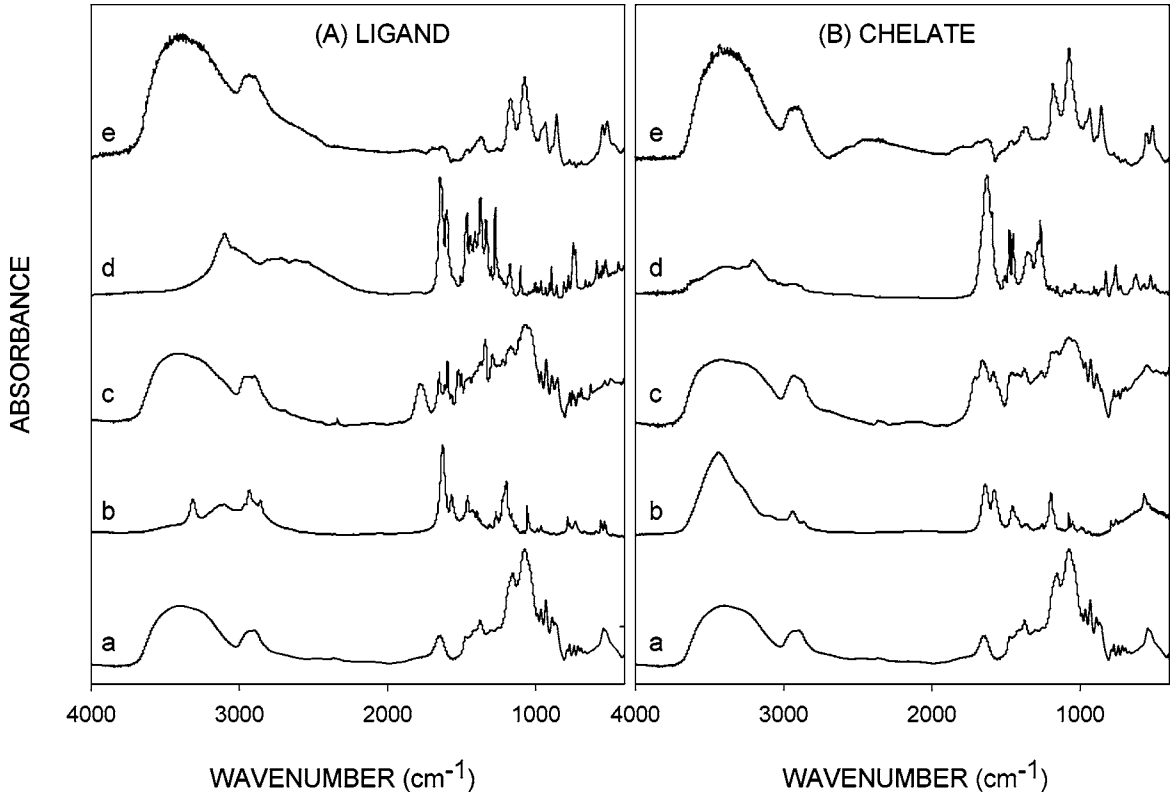

Figure 4. FTIR spectra of (A) DFOB, immobilized DFOB, EDDHA, immobilized EDDHA and (B) their complexes with Fe^{3+}: (a) Sepharose; (b) soluble DFOB; (c) immobilized DFOB; (d) soluble EDDHA; (e) immobilized EDDHA. Immobilization on (*p*-nitrophenyl)chloroformate activated Sepharose.

hydroxyl groups resulting from the coordinative bond to Fe^{3+} and to the new five-ringed structure that was formed. Binding Fe^{3+} also influenced the C═O stretching absorbance at 1628 cm^{-1}. The peak was shifted to 1639 cm^{-1}, and its intensity was reduced significantly due to the resonative O−C═N bond. Instead, new bands of C═N and C−O appeared at wavenumbers of 1580 and 1077 cm^{-1}, respectively. The relatively broad C═N peak shielded the absorbance at 1568 cm^{-1} assigned to the secondary amide that is not part of the Fe^{3+} binding.

Coupling of DFOB to activated Sepharose did not appear to influence its ability to chelate Fe^{3+} nor its binding nature. The new bands at 1580 and 1077 cm^{-1} that were distinguished upon binding Fe^{3+} by DFOB were seen with the immobilized chelate as well (at 1586 and 1078 cm^{-1}). In conclusion, the metal was bound to the immobilized DFOB through DFOB hydroxamate groups.

The FTIR spectra of EDDHA, immobilized EDDHA, and their complexes with Fe^{3+} are shown in **Figure 4**. The peak centered at 3100 cm^{-1} in the spectrum of EDDHA was assigned to the aromatic C−H stretching bands. This peak overlapped with a broad O−H stretch of the carboxylic groups at 3300−2500 cm^{-1}, N−H stretching vibrations at 3350−3310 cm^{-1}, and intermolecular hydrogen-bonded O−H stretches of the phenolic groups at 3650−3125 cm^{-1}. These peaks were significantly lowered and shifted to higher wavenumbers of 3600−3000 cm^{-1} with a maximum at 3210 cm^{-1} when EDDHA was complexed with Fe^{3+}. This change was the result of the dissociation of the functional groups involved in the Fe^{3+} binding: the phenolic and carboxylic hydroxides and the amine. When EDDHA is complexed with a metal, its interaction with water is reduced. A similar reduction in peak intensities at high frequencies was observed at the spectrum of FeDFOB.

The C−H stretching of methylene groups appeared at 2926 cm^{-1} and their bending vibrations at 1464 cm^{-1} (scissoring) and 1350−1150 cm^{-1} (twisting and wagging), and weak combination and overtone bands appeared in the 2000−1700 cm^{-1} region. The C═O band was observed at 1646 cm^{-1} due to internal hydrogen bonding that reduced the frequency of the carbonyl stretching. However, upon complexation of Fe^{3+}, the frequency of this band was reduced even more, and the strong asymmetric carboxylate anion O−C═O band appeared at 1632 and 1628 cm^{-1}.

The aromatic C═C stretching vibrations appeared around 1600 and 1464 cm^{-1}. The peak at 1464 cm^{-1} was overlapped by methylene scissoring and was split to 1476 and 1453 cm^{-1} in the spectrum of FeEDDHA. The carboxylic O−H bending at 1412 cm^{-1}, shown in the ligand spectrum, disappeared and the in-plane O−H bend at 1374, 1337, and 1331 cm^{-1}, coupled with C−H wagging, were reduced upon chelation of the metal. The strong peak at 1275 cm^{-1} was assigned to the carboxylic and phenolic C−O stretches. This peak was split into two peaks at 1284 and 1267 cm^{-1} when EDDHA was ferrated. A weak absorption band for the C−N linkage appeared at 1175 and 1102 cm^{-1}. This peak did not appear in the FeEDDHA spectrum, although the explanation for this is not clear at this point.

Immobilization of EDDHA on Sepharose gel resulted in an IR spectrum similar to that of the Sepharose. The characteristic peaks of EDDHA and FeEDDHA could hardly be detected. However, a comparison of the spectrum of the immobilized EDDHA with that of the Sepharose reveals a distinct increase in the range of 3700−2500 cm^{-1}, as compared to the peaks at 1159 and 1077 cm^{-1} resulting from C−O stretching of the polymer backbone. The aromatic C−H, carboxylic O−H, N−H, and phenolic intermolecular hydrogen-bonded O−H stretching vibrations, although shielded by the broad band of Sepharose, contributed to this increase. An increase at higher frequencies of the spectrum (3700−2800 cm^{-1}) was found for the im-

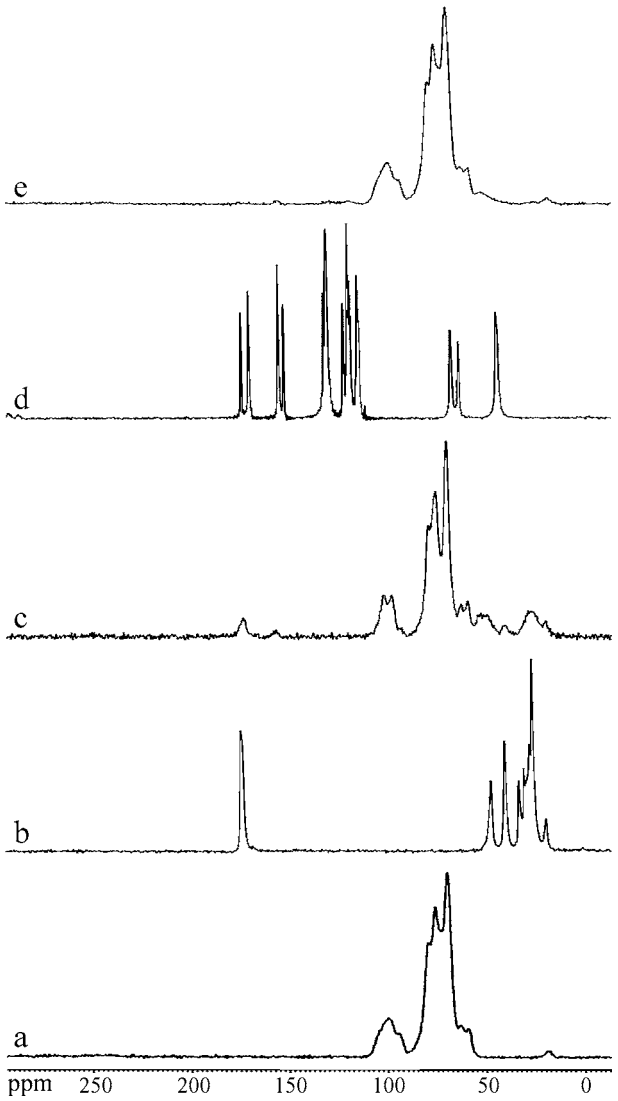

Figure 5. CPMAS ^{13}C NMR spectra of (a) Sepharose, (b) DFOB, (c) immobilized DFOB, (d) EDDHA, and (e) immobilized EDDHA (immobilization on (*p*-nitrophenyl)chloroformate activated Sepharose).

Table 2. Cross-Polarization Magic Angle Spinning (CPMAS) Nuclear Magnetic Resonance (^{13}C NMR) Spectroscopy: Peak Assignment for the Spectra of DFOB, EDDHA, and Sepharose

Chemical shift (ppm)	Assignment
DFOB	
19.5	**C**H_3–
25.9, 27.4, 30.5, 33.1	–**C**H_2–
	O ‖
40.0	–**C**H_2–**C**–
47.2	–**C**H_2–N<
	O ‖
168.4-173.7	–**C**–N<
EDDHA	
44.9	–**C**H_2–NH–
64.2, 68.2	>**C**H–NH–
117.1	aromatic **C**–H
118.9, 120.0, 122.4	aromatic **C**–H
130.7, 132.4	aromatic **C**–C
152.8, 155.4	aromatic **C**–O
	O ‖
170.4, 174.5	–**C**–OH
Sepharose	
19.5	–CH_2– alkane
59.8	–CH_2–O or >CH–O
70.0	>CH–O
76.3, 79.7	>CHO
100.0	anomeric C

mobilized FeEDDHA as for the immobilized EDDHA, but to a lesser extent.

^{13}C Solid-State NMR spectroscopy. The CPMAS ^{13}C NMR spectra of DFOB, immobilized DFOB, and Sepharose are shown in **Figure 5**. Peak identification of the ^{13}C NMR spectra of the various ligands is given in **Table 2**. In addition to the peaks originating from the polymer backbone and the ligand, the spectrum of the immobilized DFOB showed signals at 160 and 52.6 ppm. The peak at 160 ppm is assigned to the coupling bond of DFOB through its free amino group to the Sepharose. The changes in the spectrum of immobilized EDDHA could hardly be detected, possibly due to low ligand density on the gel (**Figure 5**). Zooming in on that part of the spectrum, we observed very small peaks at 155 and 52.8 ppm. The peak at around 155 ppm could be the result of the phenyl group or the carbonate bond that is formed upon coupling of EDDHA to the matrix through its amine or hydroxyl group. The peak at 53 ppm is assigned to the deshielding of the (α-)carbon induced by the deprotonation of the amino group attached to the activated gel. This indicates that in EDDHA as well as in DFOB the attachment to the gel is through the amino group.

DFOB contains three hydroxamic acid groups and a terminal free amino group. It coordinates with Fe^{3+} through its three hydroxamates, forming an octahedral Fe chelate. The stability of the Fe^{3+} complex is very high (log $K = 31.4$ (*14*, *27*)). This high stability is attributed not only to the high coordinative energy of the hydroxamic acid for Fe(III) but also to the number and spacing of the coordinative groups. Evaluation of these Fe scavengers in living organisms has shown that the spacing of hydroxamic acids adjusts so that the three hydroxamic acids of the siderophore precisely fit the required octahedral coordination sphere of the Fe (*13*). As apparent from FTIR and NMR analyses, these properties of DFOB remain unchanged by immobilization on PNPCF activated Sepharose.

Fe-Binding Isotherms: Thermodynamics of Formation of the Metal Complexes. The affinity of Fe to the immobilized ligand was evaluated by plotting the binding (adsorption) isotherm, in which the amount of the ion bound to the polymer is plotted against the concentration of soluble Fe^{3+} (**Figure 6**). Isotherms for the immobilized DFOB were determined in the presence of 1 mM HEDTA at pH values of 4.0, 5.5, 6.4, 7.3, and 9.1 and at 0.1 M ionic strength. All curves are concave to the soluble ion concentration ordinate, indicating that the binding is not cooperative. The H-type isotherm observed for the immobilized DFOB showed a very high affinity of Fe^{3+} to the ligands and saturable binding to the immobilized DFOB. The

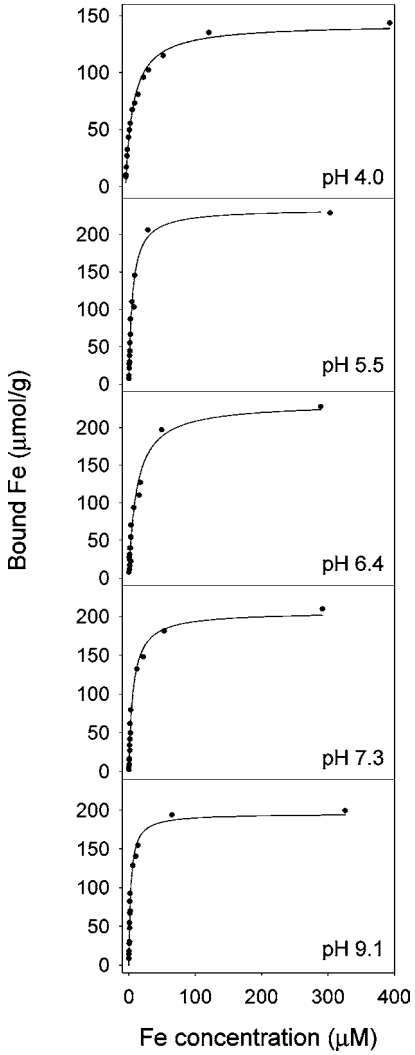

Figure 6. Binding isotherm of Fe^{3+} to DFOB immobilized on (*p*-nitrophenyl)chloroformate activated Sepharose at various pH levels.

Table 3. Langmuir-Binding Model Parameters of Fe^{3+} Binding Isotherms by DFOB Immobilized on (*p*-Nitrophenyl)chloroformate Activated Sepharose

pH	K_1[a]	K_2[b]	K_1K_2[c]	R^2[d]
4.0	142.8	0.086	12.3	0.990
5.5	234.4	0.174	40.9	0.977
6.4	233.0	0.085	19.5	0.973
7.3	205.9	0.155	31.9	0.984
9.1	195.6	0.335	65.5	0.969

[a] Number of binding sites (μmol/g). [b] A constant reflecting the binding energy (μM^{-1}). [c] The slope of the linear part of the curve. [d] Direct fitting of the data to the curve.

degree to which the results fit the Langmuir model (equation) is summarized in **Table 3**.

The values of K_1 and K_2 represent the concentration of binding sites and the binding energy constant, respectively. The concentration of binding sites was found to be in the range of 143−234 μmol/g and was pH dependent. The K_2 constant, which is related to the affinity, that is the binding energy, varied between 0.016 and 0.335 μM^{-1}. It should be noted that the Langmuir adsorption equation assumes a monolayer adsorption on a uniform surface with no interactions between adsorbed molecules (*10*).

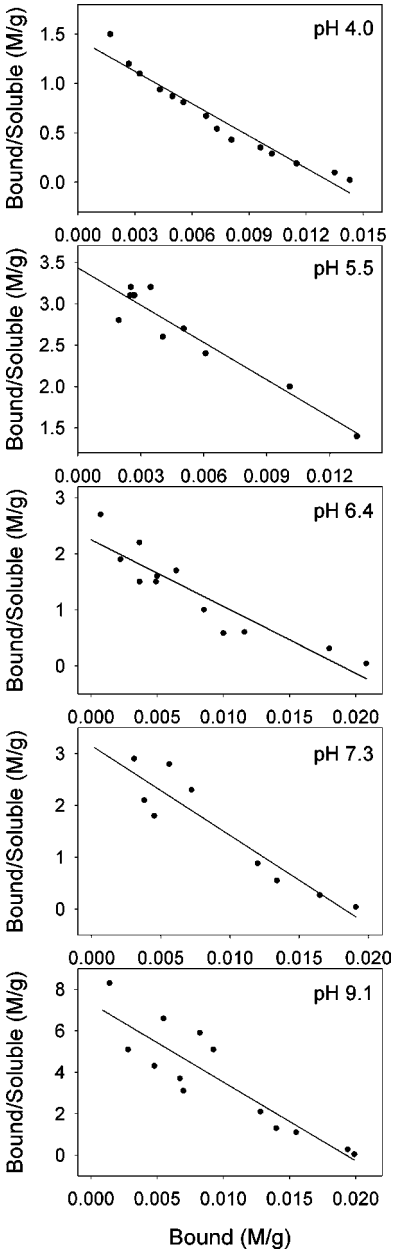

Figure 7. Scatchard plots of DFOB immobilized on (*p*-nitrophenyl)-chloroformate activated Sepharose with Fe^{3+} at various pH levels.

Table 4. Parameters of a Scatchard Model Analysis of Fe^{3+} Binding Isotherms by DFOB Immobilized on (*p*-Nitrophenyl)chloroformate Activated Sepharose

pH	K''[a]	K_{HEDTA}	K'[b]	N[c]	R^2	K' ligand competition
4.0	110.9	$10^{12.7}$	$10^{14.7}$	133	0.949	$10^{14.0}$–$10^{14.8}$
5.5	152.5	$10^{16.5}$	$10^{18.7}$	248	0.907	$10^{18.4}$–$10^{18.8}$
6.4	118.5	$10^{18.7}$	$10^{21.0}$	209	0.850	$10^{20.7}$–$10^{21.2}$
7.3	171.7	$10^{20.4}$	$10^{22.6}$	201	0.870	$10^{22.0}$–$10^{22.6}$
9.1	381.1	$10^{24.3}$	$10^{26.9}$	193	0.800	$10^{26.0}$–$10^{26.9}$

[a] The combined apparent stability constant. [b] Apparent stability constant of immobilized DFOB. [c] Concentration of binding sites (μmol/g).

Scatchard plots of the binding isotherms are shown in **Figure 7**. The constants K'' for the system containing immobilized DFOB, HEDTA, and Fe^{3+} at various pHs were calculated from the slope of the linear curve fits. These results are summarized in **Table 4**. The formation constant of the immobilized complex,

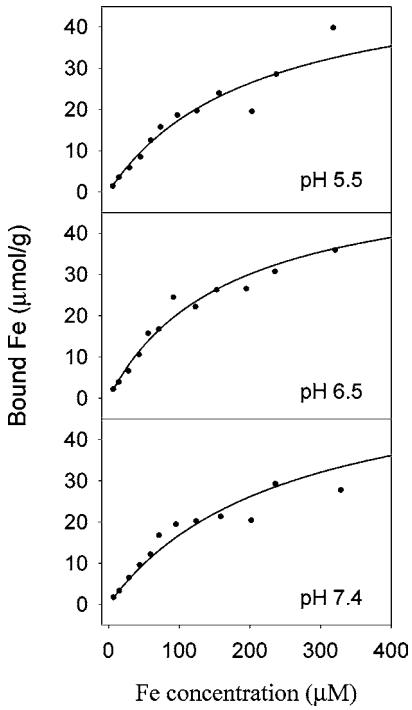

Figure 8. Binding isotherm of Fe^{3+} to EDDHA immobilized on (*p*-nitrophenyl)chloroformate activated Sepharose at various pH levels.

K′, was calculated from multiplication of *K″* by the K_{app} value of HEDTA.

The apparent stability constant, *K′*, of the immobilized DFOB increased with increasing pH (**Table 4**). The number of available binding sites was calculated from the intercept of the curves (**Figure 7**) and was also found to be pH-dependent, with a maximum value of 248 mmol/g at pH 5.5. The changes are probably the result of competition with hydrogen ions at pHs lower than 5.5 and with Fe hydroxides at higher pHs.

Each point on the curves shown in **Figure 6** represents an equilibrium state between the immobilized ligand, the soluble ligand, the metal, and their complexes, where the total concentrations of both soluble and immobilized ligands are constant and the total metal concentration is increasing. The ranges of values obtained for *K′* according to ligand−ligand competition were $10^{14.1}-10^{14.5}$, $10^{18.6}-10^{18.8}$, $10^{20.6}-10^{21.2}$, $10^{22.1}-10^{22.6}$, and $10^{26.4}-10^{26.9}$ for pH levels of 4.0, 5.5, 6.4, 7.3, and 9.1, respectively. A reference for the log β values used in the calculations of K_{app} for Fe(III) and the competitive ligand, HEDTA, was given by Martell and Smith (*27*). The *K′* values determined using eq 5 are in accordance with those found using the Scatchard analysis (Table 4).

Binding isotherms of Fe^{3+} to immobilized EDDHA at pH levels of 5.5, 6.5, and 7.4 are shown in **Figure 8**. The L-type isotherms indicate high affinity of the metal to EDDHA immobilized on Sepharose. However, the affinity was not as high as for the immobilized DFOB. This is supported by the parameters that were found according to the Langmuir equation (**Table 5**). The bonding energy constant, K_2, was in the range of 0.004−0.006 μM^{-1}, which is much lower than that found for the Fe^{3+} binding to immobilized DFOB (**Table 3**). Moreover, the maximum capacity of the binding sites in immobilized EDDHA approached 60 μmol of Fe^{3+}/g and was significantly lower than that exhibited by the immobilized DFOB (about 250 μmol/g).

The constants for the system containing both competitive ligands and Fe^{3+} were calculated using Scatchard plots (**Figure 9**), and the apparent formation constants, *K′*, of the immobilized EDDHA with the metal were determined accordingly. The results of the Scatchard analysis exhibited an increase in K_{app} for the Fe^{3+} bound to immobilized EDDHA with increasing pH (**Table 5**). The same trend was found for Fe^{3+} bound to immobilized DFOB. Calculation of these constants using the ligand competition method resulted with $10^{17.1}-10^{17.4}$, $10^{19.5}-10^{19.7}$ and $10^{21.1}-10^{21.4}$ for Fe^{3+} bound to immobilized EDDHA at pH levels of 5.5, 6.5, and 7.4, respectively. The values are in accordance with those found using the Scatchard analysis (**Table 5**).

Table 5. Parameters of Fe^{3+} Binding Isotherms by EDDHA Immobilized on (*p*-Nitrophenyl)chloroformate Activated Sepharose

	Langmuir-binding model			Scatchard analysis			
pH	K_1[a]	K_2[b]	R^2	K''[c]	K'[d]	N[e]	R^2
5.5	53.6	0.005	0.930	4.75	$10^{17.2}$	56.1	0.853
6.5	55.3	0.006	0.974	5.80	$10^{19.7}$	54.4	0.960
7.4	58.5	0.004	0.925	5.09	$10^{21.7}$	53.3	0.885

[a] A constant reflecting the number of binding sites (μmol/g). [b] A constant reflecting the binding energy (μM^{-1}). [c] The combined apparent stability constant. [d] Apparent stability constant of immobilized EDDHA (M^{-1}). [e] Concentration of binding sites (μmol/g).

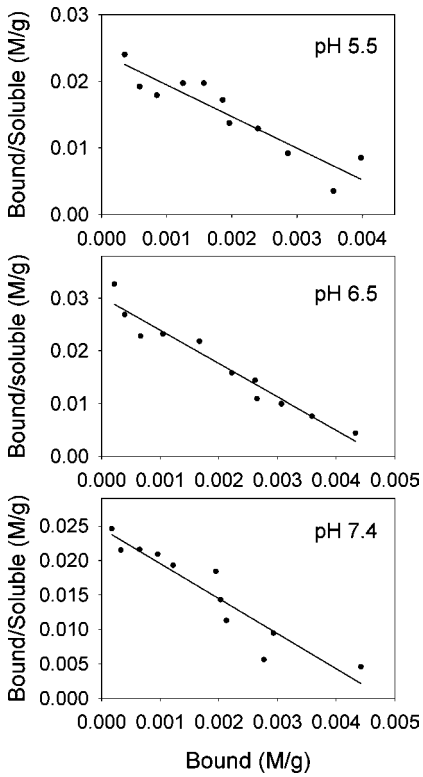

Figure 9. Scatchard plots of EDDHA immobilized on (*p*-nitrophenyl)-chloroformate activated Sepharose with Fe^{3+} at various pH levels.

The capacity of Fe^{3+} binding was analyzed according to Scatchard analysis. It was found to be within the range of 53−56 μmol/g with a maximum at pH 5.5. These values were close to the values that were found using the Langmuir equation, although in the latter case the maximum was obtained at pH 7.4 (**Table 5**).

Since attaching the ligand to the activated matrix was performed at high ligand concentrations, ligand density on the gel and, therefore, its concentration in the system were difficult to evaluate. The use of the Scatchard analysis to determine the apparent stability constant eliminates the need to determine the

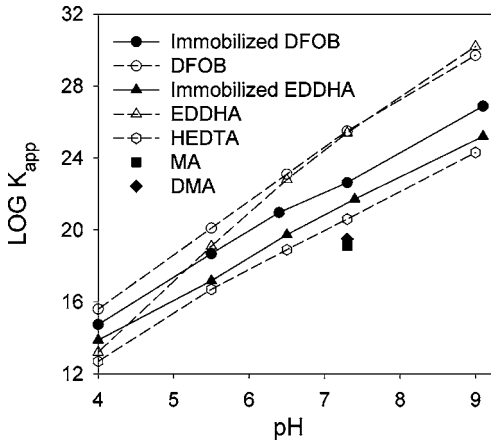

Figure 10. Apparent stability constant, K_{app}, for Fe^{3+} binding to DFOB immobilized on (*p*-nitrophenyl)chloroformate activated Sepharose and other known ligands and phytosiderophores (MA, mugineic acid; DMA, deoxymugineic acid) as a function of pH.

total immobilized-ligand concentration and gives additional information regarding the maximal binding capacity for metals under certain conditions. This approach has also been used and found to be useful by many researchers in studies on metal binding to macromolecules having an unknown structure yet known charge distribution functions (*10*, *28*).

A graphic description of the change in the K_{app} values of the immobilized DFOB and immobilized EDDHA with pH as determined by Scatchard analysis (in comparison with known chelates) is given in **Figure 10**. The K_{app} values of the immobilized chelates are lower than those of the soluble ones. The difference in K_{app} between DFOB and immobilized DFOB and between EDDHA and immobilized EDDHA increased with pH, suggesting a change in the protonation constants of the immobilized chelators as compared with the soluble ligand.

This assumption is in contrast with the hypothesis of Feng et al. (*29*) and needs further investigation. These researchers used the ligand competition method to determine stability constants of Fe^{3+}−ligand complexes on insoluble polymeric matrixes. For DFOB immobilized on CNBr-activated Sepharose, they assumed the same protonation constants as for the soluble ligand and found a value of $10^{26.6}$ for the overall stability constant ($\beta_{ML'}$) with Fe^{3+}. The species L'^{3-} and FeL'^{0} do not represent the only possible species of the immobilized ligand and its ferric complex (*11*). It is also unlikely that bound and free ligands will exhibit the same protonation constants. This statement is also supported by the fact that the Fe^{3+} binding constants are different for free and bound ligands. Therefore, as was mentioned earlier, the apparent stability constant is a more useful tool for the evaluation of the ability of chelating agents to compete for Fe^{3+} than the overall stability constant.

The reduction in K_{app}, resulting from the immobilization on the activated Sepharose, is more significant in EDDHA than in DFOB. The attachment of the ligand to the PNPCF activated Sepharose occurs via the amine group (*23*). DFOB has a terminal free amino group that is covalently bound to the gel. As became clear from the FTIR analysis (**Figure 4**), binding groups preserve their Fe^{3+} binding nature. In contrast to DFOB, EDDHA is attached to the matrix through at least one of its two amine groups that is participating in Fe^{3+} binding. Therefore, its chelating ability is much more influenced by the immobilization process, resulting in significantly lower formation constants with the metal.

The efficacies of Sepharose (*30*) or clay bound chelate (*31*) in providing Fe^{3+} to plants were recently reported. We wish to stress here that the lower K_{app} which was found for Fe^{3+} bound to the immobilized DFOB as compared to its soluble form could actually be beneficial, by being instrumental in facilitating Fe uptake by plants. Higher plants use strategies of reduction, acidification, and chelation to utilize Fe. Dicots and nongrass monocots reduce complexed Fe^{3+} to Fe^{2+}, which is the form taken up by the roots. In addition, dicots release protons to the rhizosphere and lower the pH. The decrease in pH increases the solubility of Fe in the soil solution. A different mechanism for acquiring Fe operating in grasses is the release of phytosiderophores (*32*). The uptake of Fe from rhizoferrin, a microbial siderophore by barley and corn, has been shown to occur via an indirect mechanism that involves ligand exchange between rhizoferrin and the phytosiderophores (*33*). According to calculations of K_{app} for synthetic and microbial chelators such as EDTA, EDDHA, DFOB, and pseudobactin with Fe^{3+} at pH 7.3, it was suggested that their values are too high for effective ligand exchange (*34*). Lowering the K_{app} by immobilization of DFOB and EDDHA by 3- and 5-fold, respectively (**Figure 10**), can be significant for ligand exchange reactions with phytosiderophores (i.e. mugineic acid and deoxymugineic acid) and Fe uptake in Poacea species. This issue should be further investigated, and the ability of these chelates to serve as Fe carriers to plants operating by both strategy I and strategy II is currently investigated in our laboratory. However, the immobilized chelate approach shown here should be further developed and examined in soil cultures. Once its stability constants with other metals prevailing in soil solution is determined, its species distribution in soil can be predicted using computational programs (e.g. GEOCHEM-PC (*35*)). In addition, its properties should be optimized mostly with regard to its ability to serve as an Fe source to plants and its resistance to removal processes such as leaching and photochemical and biological degradation. An emphasis should also be given to the cost of a new product developed along the proposed lines, including testing of other bound ligands (e.g. rhizoferrin). Different techniques of application in the field and cheaper supports should also be tried out.

Abbreviations Used. DFOB, Desferrioxamine B; EDDHA, ethylendiaminebis(*o*-hydroxyphenylacetic acid); HEDTA, ethylenediaminetriacetic acid; EDTA, ethylenediaminetetraacetic acid; DTPA, diethylenetriaminepentaacetic acid; MA, mugineic acid; DMA, deoximugineic acid; PNPCF, *p*-nitrophenylchloroformate; TSTU, *O*,*N*-succinimidyl-*N*,*N*,*N*′,N′-tetramethyluronium tetrafluoroborate; DMAP, (dimethylamino)pyridine; K_{app}, apparent stability constant.

ACKNOWLEDGMENT

We wish to thank Meir Wilchek, of the Weizmann Institute of Science, for sharing with us his knowledge on immobilization processes. We also wish to thank Moshe Shenker of The Hebrew University of Jerusalem for his helpful comments and Patrick Hatcher of The Ohio State University for allowing us to use his ^{13}C solid-state NMR.

LITERATURE CITED

(1) Compañó, R.; Ferrer, R.; Guiteras, J.; Part, M. D. Specrofluorimetric detection of zinc and cadmium with 8-(benzenesulfonamido)-quinoline immobilized on a polymeric matrix. *Analyst* **1994**, *119*, 1225−1228.

(2) Kantipuly, C.; Katragadda, S.; Chow, A.; Gesser, H. D. Chelating polymers and related supports for separation and preconcentration of trace metals. *Talanta* **1990**, *37*, 491−517.

(3) Lancaster, H. L.; Marshall, G. D.; Gonzalo, E. R.; Ruzicka, J.; Christian, G. D. Trace metal atomic absorption spectrometric analysis utilizing sorbent extraction on polymeric-based supports and renewable reagents. *Analyst* **1994**, *119*, 1459−1465.
(4) Shani, S. K.; Reedijk, J. Coordination chemistry of chelating resins and ion exchangers. *Coord. Chem. Rev.* **1984**, *59*, 1−139.
(5) Tyllianakis, P. E.; Kakabakos, S. E.; Evangelatos, G. P.; Ithakissios, D. S. Direct colorimetric determination of solid-supported functional groups and ligands using bicinchoninic acid. *Anal. Biochem.* **1994**, *33*, 335−340.
(6) Rombolà, A. D.; Bruggemann, W.; López-Millán, A. F.; Tagliavini, M.; Abadía, J.; Marangoni, B.; Moog, P. R. Biochemical responses to iron deficiency in kiwifruit (Actinidia deliciosa). *Tree Physiol.* **2002**, *22*, 869−875.
(7) Shenker, M.; Chen, Y. Increasing iron availability to crops: fertilizers, organo-fertilizers, and biological approaches. *Plant Soil*, in press.
(8) Wallace, A.; Mueller, R. T.; Lunt, O. R.; Ashcroft, R. T.; Shannon, L. M. Comparisons of five chelating agents in soils, in nutrient solutions, and in plant responses. *Soil Sci.* **1955**, *80*, 101−108.
(9) Chen, Y.; Barak, P. Iron nutrition of plants in calcareous soils. *Adv. Agron.* **1982**, *35*, 217−240.
(10) Stevenson, F. J. *Humus Chemistry*; Wiley: New York, 1994.
(11) Shenker, M.; Hadar, Y.; Chen, Y. Stability constants of the fungal siderophore rhizoferrin with various microelements and calcium. *Soil Sci. Soc. Am. J.* **1996**, *60*, 1140−1144.
(12) Anderegg, v. G.; L'Eplattenier, F.; Schwarzenbach, G. Hydroxamatkomplexe II. Die anwendung der pH-methode. *Helv. Chim. Acta* **1963**, *46*, 1400−1408.
(13) Winston, A.; Kirchner, D. Hydroxamic acid polymers. Effect of structure on the selective chelation of iron in water. *Macromolecules* **1978**, *11*, 597−603.
(14) Schwarzenbach, G.; Schwarzenbach, K. *Helv. Chim. Acta* **1963**, *46*, 1390−1400.
(15) Scatchard, G. The attractions of proteins for small molecules and ions. *Ann. N. Y. Acad. Sci.* **1949**, *51*, 660−672.
(16) Kawakami, H.; Lonnerdal, B. Isolation and function of a receptor for human lactoferrin in human fetal intestinal brush-border membranes. *Am. J. Physiol.* **1991**, *261*, G841-G846.
(17) Tachezy, J.; Kulda, J.; Bahnikova, I.; Suchan, P.; Razga, J.; Schrevel, J. Trichomonas foetus: Iron acquisition from lactoferrin and transferrin. *Exp. Parasitol.* **1996**, *83*, 216−228.
(18) Bowen, B. J.; Morgan, E. H. Anemia of the Belgrade rat: evidence for defective membrane transport of iron. *Blood* **1987**, *70*, 38−44.
(19) Nir, S.; Peled, R.; Lee, K. D. Analysis of particle uptake by cells: binding to several receptors, equilibrium time, endocytosis. *Colloids Surf.* **1994**, *89*, 45−57.
(20) Bernos, E.; Girardet, J. M.; Humbert, G.; Linden, G. Role of the O-phosphoserine clusters in the interaction of the bovine milk alphas1-, beta-, kappa-caseins and the PP3 component with immobilized iron (III) ions. *Biochim. Biophys. Acta* **1997**, 149−159.
(21) Fitch, A.; Stevenson, F. J.; Chen, Y. Complexation of Cu(II) with a soil humic acid: Response characteristic of the Cu(II) ion-selective electrode and ligand concentration effects. *Org. Geochem.* **1986**, *9*, 109−116.
(22) Kohn, J.; Wilchek, M. The use of cyanogen bromide and other novel cyanylating agents for the activation of polysaccharide resins. *Appl. Biochem. Biotechnol.* **1984**, *9*, 285−305.
(23) Wilchek, M.; Miron, T. Immobilization of enzymes and affinity ligands onto agarose via stable and uncharged carbamate linkages. *Biochem. Int.* **1982**, *4*, 629−635.
(24) Wilchek, M.; Miron, T. Polymers coupled to agarose as stable and high capacity spacers. *Methods Enzymol.* **1974**, *34*, 72−6.
(25) Wilchek, M.; Oka, T.; Topper, Y. J. Structure of a soluble superactive insuline is revealed by the nature of the complex between cyanogen-bromide-activated Sepharose and amines. *Proc. Natl. Acad. Sci. U.S.A.* **1975**, *72*, 1055−1058.
(26) Jost, R.; Miron, T.; Wilchek, M. The mode of adsorption of proteins to aliphatic and aromatic amines coupled to cyanogen bromide-activated agarose. *Biochim. Biophys. Acta* **1974**, *362*, 75−82.
(27) Martell, A. E.; Smith, R. M. *Critical Stability Constants*; Plenum Press: New York, 1977.
(28) Kaschl, A.; Römheld, V.; Chen, Y. Cadmium binding by fractions of dissolved organic matter and humic substances from municipal solid waste compost. *J. Environ. Qual.* **2002**, *31*, 1885−1892.
(29) Feng, M.; Van Der Does, L.; Bantjes, A. Iron(III) chelating resins. VI. Stability constants of iron(III)-ligand complexes on insoluble polymeric matrixes. *J. Appl. Polym. Sci.* **1995**, *56*, 1231−1237.
(30) Yehuda, Z.; Hadar, Y.; Chen, Y. Immobilized EDDHA and DFOB as iron carriers to cucumber plants. *J. Plant Nutr.* **2003**, *26*, 2043−2056.
(31) Siebner-Freibach, H.; Hadar, Y.; Chen, Y. Siderophores sorbed on Ca-montmorilonite as an iron source for plants. *Plant Soil* **2003**, *251*, 115−124.
(32) Marschner, H.; Römheld, V.; Kissel, M. Different strategies in higher plants in mobilization and uptake of iron. *J. Plant Nutr.* **1986**, *9*, 695−713.
(33) Yehuda, Z.; Shenker, M.; Römheld, V.; Marschner, H.; Hadar, Y.; Chen, Y. The role of ligand exchange in the uptake of iron from microbial siderophores by gramineous plants. *Plant Physiol.* **1996**, *112*, 1273−1280.
(34) Yehuda, Z.; Shenker, M.; Hadar, Y.; Chen, Y. Remedy of chlorosis induced by iron deficiency in plants with the fungal siderophore rhizoferrin. *J. Plant Nutr.* **2000**, *23*, 1991−2006.
(35) Parker, D. R.; Norvell, W. A.; Chaney, R. L. GEOCHEM-PC: A chemical speciation program for IBM and compatible personal computer. In *Chemical Equilibrium and Reaction Models*; Loeppert, R. H., Schwab, A. P., Goldberg, S., Eds.; SSSA/ASA Special Publications: Madison, WI, 1995; Vol. 42, pp 253−270.

Received for review February 19, 2003. Revised manuscript received July 18, 2003. Accepted July 21, 2003. We wish to thank the Horowitz Foundation for their financial support.

JF034159H